Available online at www.sciencedirect.com
SCIENCE DIRECT®

Journal of the European Ceramic Society 23 (2003) 2841–2848
www.elsevier.com/locate/jeurceramsoc

Grain boundary segregation in oxide ceramics

P. Wynblatt*, G.S. Rohrer, F. Papillon

Department of Materials Science and Engineering, Carnegie Mellon University, Pittsburgh PA 15213, USA

Abstract

The factors which control grain boundary segregation in oxide ceramics are reviewed. These include grain boundary energy, cation–cation interactions, impurity cation size, as well as electrostatic interactions with the grain boundary space charge. In addition, an approach for measuring grain boundary segregation in those materials, as a function of the five macroscopic parameters of grain boundary character, is described. This experimental method relies on the coupled application of orientation imaging microscopy and scanning Auger spectroscopy.

Keywords: Grain boundaries; Interfaces; MgO; Oxides

1. Introduction

The term interfacial segregation (or interfacial adsorption) refers to the localized change (increase) in the concentrations of one or more components at interfaces in multi-component systems, in relation to their concentrations in the adjacent bulk phases. Segregation is driven by the decrease in interfacial free energy that accompanies the adsorption process, as was first pointed out by Gibbs over a century ago.[1] The topic of interfacial segregation has received considerable discussion in the literature. Of the various possible interfaces of interest to materials scientists, solid–vapor interfaces (i.e. free surfaces) have perhaps been most comprehensively studied. Also, among the various materials classes, interfaces in metallic alloys have been most thoroughly investigated.

From an experimental perspective, interfacial segregation has been studied most often by surface analytic techniques. This approach is obviously most applicable to free surfaces, which are readily accessible by this type of technique. In the case of buried interfaces (such as grain or interphase boundaries) the application of surface analysis techniques generally requires conversion of the buried interface into a surface by interfacial fracture. However, not all buried interfaces are necessarily amenable to easy fracture. As a result, interfaces which are not embrittled by the presence of a segregant, and which do not naturally part along internal interfaces, have generally received less comprehensive study. Experimental approaches that lend themselves to the investigation of interfacial segregation, without the need for fracturing the interface, include atom probe field ion microscopy,[2] analytical electron microscopy,[3] and secondary ion mass spectrometry.[4]

Historically, the first studies of interfacial segregation focused on the problem of grain boundary (GB) embrittlement by trace element segregation in steel.[5] Since that time, considerable progress has been made in understanding interfacial segregation of impurities at GBs as well as other interfaces. In the context of ceramic materials, GB segregation may modify many important properties of technological interest. It may affect mechanical properties such as creep and fracture, provide a means for controlling the microstructure through its effect on GB mobility, determine intergranular corrosion behavior, and modify electrical properties.

In this paper, we will begin by discussing the various factors that contribute to the driving force for GB segregation in ionic materials, and then proceed to describe an approach for studying the phenomenon at the GBs of such materials.

2. Fundamental concepts

2.1. GB character

A GB is an interface in a single-phase material, as shown schematically in Fig. 1. It represents the region of

* Corresponding author. Tel.: +1-412-268-8711; fax: +1-412-268-7596.
E-mail address: pw0l@andrew.cmu.edu (P. Wynblatt).

0955-2219/03/$ - see front matter © 2003 Elsevier Ltd. All rights reserved.
doi:10.1016/S0955-2219(03)00308-X

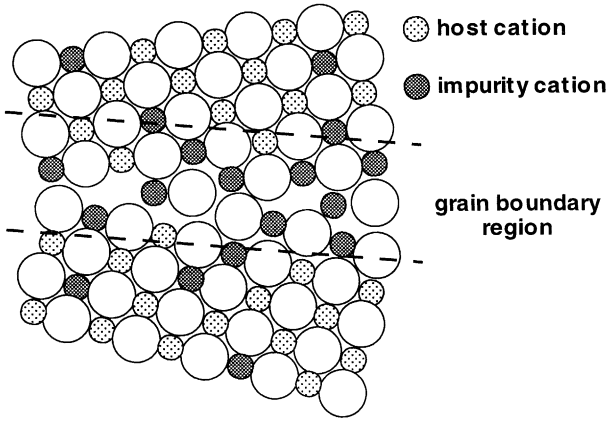

Fig. 1. Schematic of segregated GB, in which dark circles represent segregated solute ions.

transition between two crystalline domains (grains) which differ from each other in crystallographic orientation. The properties of a GB (e.g., its structure, energy, mobility, composition, etc.) are expected to depend on five macroscopic degrees of freedom (DoFs), and possibly on three additional microscopic DoFs. The macroscopic DoFs are generally specified by (a) the three angles which allow rotation of the crystallographic axes of one grain adjacent to the GB into the axes of the other adjacent grain, and (b) the two angles which define the inclination of the GB with respect to the two grains. The microscopic DoFs represent small adjustments in the relative positions of the two grains, and may lead to further reduction in GB energy, and/or small changes in other properties. For an equilibrated boundary where the five macroscopic DoFs, as well as the temperature, pressure, and composition, are all fixed, the three microscopic parameters are assumed to be constant. The DoFs are parameters which define GB character.

2.2. Gibbsian adsorption

According to Gibbs,[1] GB adsorption in a phase containing N components, modifies the GB energy, γ, by:

$$\mathrm{d}\gamma = -\sum_{i}^{N} \Gamma_i \mathrm{d}\mu_i \tag{1}$$

where Γ_i is the adsorption of component i (i.e. the excess number of moles of i per unit area of GB) and μ_i is the chemical potential of the ith component. The adsorption is defined as:

$$\Gamma_i = \frac{(n_i - X_i^b n)}{A} \tag{2}$$

where n_i is the total number of moles of component i and n is the total number of moles of all components, in a system comprised of two grains of a phase of bulk composition X_i^b which contains a GB of area A. This assumes that the two grains have uniform composition X_i^b up to a hypothetical "dividing surface" located in the vicinity of the GB.

Consider a substitutional solid solution consisting of two components, a solvent (species 1) and an interfacially active solute (species 2). If the concentration of the solute is low enough that the solution may be considered to behave according to Henry's law, then Eq. (1) may be approximated as:

$$\left(\frac{\mathrm{d}\gamma}{\mathrm{d}X_2^b}\right)_T = -\frac{RT\Gamma_2}{X_2^b} \tag{3}$$

where X_2^b is the mole fraction of solute, and R and T are the gas constant and absolute temperature, respectively. Classical thermodynamics do not provide the relationship between Γ_2 and X_2^b needed to integrate Eq. (3). However, approximate relations between those quantities, as described in the following section, are available to perform the integration and obtain estimates of the GB energy change resulting from adsorption.

2.3. Interfaces in ionic materials

The compositional variation associated with equilibrium adsorption at interfaces in elemental solid solutions (such as metallic or elemental semiconductor solutions) tend to be confined to a few (typically three or four) atomic distances. In contrast, in ionic solids, the interfacial composition variation may extend over considerably larger distances (up to $\sim$100 nm). Furthermore, near-interface deviations from ideal stoichiometry can occur even in pure ionic compounds.

In an ideal, ionic crystal containing Schottky defects (which is large enough that the presence of interfaces can be neglected) the equilibrium site fractions of cation and anion vacancies (V_+ and V_-) may be expressed as:

$$V_+ \cdot V_- = \exp\left\{-\frac{G_\mathrm{s}}{kT}\right\} \tag{4a}$$

where G_s is the free energy of formation of a Schottky pair. Assuming the compound remains stoichiometric and charge neutral, the fractions of cation and anion defects will be equal, thus:

$$V_+ = V_- = \exp\left\{-\frac{G_s}{2kT}\right\} \tag{4b}$$

However, as was originally pointed out by Frenkel [6] the formation energies of individual point defects that make up charge-compensating defect pairs need not be identical. Whereas the requirement of charge neutrality constrains these defects to have stoichiometric ratios in the bulk, this constraint is relaxed near point defect sources (or sinks) where the defect of lower formation energy will predominate. Such defect sources include interfaces as well as dislocations. The resulting

imbalance of the numbers of oppositely charged defects in the vicinity of interfaces leads to a space charge region, which is compensated by excess anions or cations at the interface. A schematic of the charge density distribution in the vicinity of an interface in a pure (NaCl-like) ionic solid is shown in Fig. 2. As illustrated in the figure, the interface can be considered to consist of two regions which deviate in composition from the stoichiometric bulk: the *physical interface*, which is only a few interatomic distances in width, and the *space charge region* which can extend from a few nanometers to as much as 100 nm.

Since the excess or deficiency of cations and anions in the physical interface of a pure ionic compound is exactly compensated within the adjacent space charge region, there is no overall interfacial excess of these species, and Gibbsian adsorption is therefore absent. However, this is not the case when solutes are present. Subsequent to Frenkel's treatment, several refinements to the theory of ionic interfaces have been proposed.[7–10] These have addressed the near-interface distribution of both isovalent and aliovalent impurities in simple NaCl-like compounds, and will be discussed below. More recently, the theory has also been extended to perovskite materials (containing two cations).[11] In this paper, we will focus primarily on how these concepts apply to simple oxides such as MgO.

In a pure (NaCl-like) ionic compound, the equilibrium site fractions of cation and anion vacancies, as a function of distance from the physical interface, d, are given by:

$$V_+(d) = \exp\left\{-\frac{G_+ - e\Phi(d)}{kT}\right\} \tag{5a}$$

$$V_-(d) = \exp\left\{-\frac{G_- + e\Phi(d)}{kT}\right\} \tag{5b}$$

where $G_+ + G_- = G_s$

Here, G_+ and G_- are the respective free energies of formation of cation and anion vacancies, e is the absolute value of the electronic charge, $\Phi(d)$ is the electrostatic potential at d, and the thickness of the physical interface is assumed to be vanishingly small. Following Kliewer and Koehler,[8] we set the potential to zero at $d=0$. Then, since $V_+ = V_-$ far from the interface, Eqs. (5a) and (5b) yield:

$$e\Phi_\infty \equiv e\Phi(\infty) = \frac{1}{2}(G_+ - G_-) \tag{6}$$

Thus, the internal potential far from the interface, Φ_∞, is simply related to the difference between the energies of formation of the two defects. Other treatments have defined the internal potential to be zero, and have expressed the results in terms of the surface potential, Φ_0; those potentials are related by $\Phi_\infty = -\Phi_0$.

2.4. Free energy of segregation

In the simplest case of a binary solid solution consisting of two atomic species (e.g., a metallic or elemental semiconductor solid solution), the free energy of segregation may be defined as the free energy change associated with the exchange of a solute atom lying in the bulk, far from the interface, with a solvent atom lying in the interface. The free energy of segregation, ΔG_s, may then be expressed in terms of the mole fractions of the solute and solvent, as:

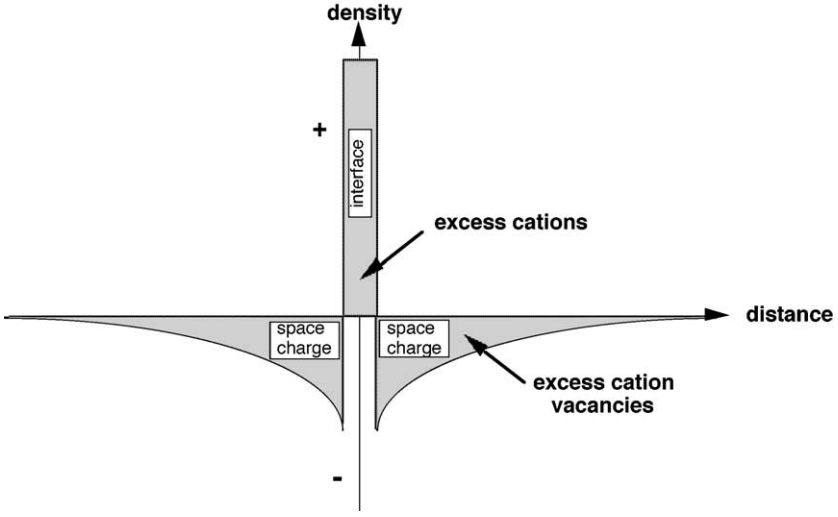

Fig. 2. Schematic of the near-interface region of a pure ionic solid such as NaCl, where $G_+ < G_-$. The figure illustrates the positive charge density at the physical interface due to excess cation adsorption which compensates for the excess cation vacancies in the space charge regions on either side of the interface (see text).

$$\ln\left(\frac{X_2^{\varphi}}{X_1^{\varphi}}\right) = \ln\left(\frac{X_2^{b}}{X_1^{b}}\right) - \frac{\Delta G_s}{RT} \tag{7}$$

where X_i^b and X_i^{φ} are the mole fractions of species i in the bulk (b) and the interface (φ) respectively. The symbol φ representing the interface should not be confused with Φ used for the potential. Expressions such as Eq. (7) provide relationships between the interfacial adsorption and the bulk composition (not provided by Gibbs) and can be obtained from approximate statistical thermodynamic treatments.[12]

For an oxide solution, it is convenient to define the free energy of segregation as that associated with the exchange of a "molecular unit" of solute in the bulk with a corresponding unit of solvent in the interface. In the event that the solid solution consists of isovalent cations (e.g., a solution of CaO in MgO) in which the solute cations occupy the same type of sites as solvent cations, exchange of a molecular unit is of course equivalent to an exchange of the cations. In principle, Eq. (7) applies to that case for the mole fraction of solute within the physical interface.

Most models of interfacial segregation, whether developed for the case of ionic or non-ionic solids, have made use of a regular solution framework, in which Eq. (7) is simplified to:

$$\ln\left(\frac{X_2^{\varphi}}{X_1^{\varphi}}\right) = \ln\left(\frac{X_2^{b}}{X_1^{b}}\right) - \frac{\Delta H_s}{RT} \tag{8}$$

Here, the (non-configurational) entropy of segregation is assumed to vanish. For the case of non-ionic solid solutions, the enthalpy of segregation has generally been taken[13] to consist of three contributions: an interfacial energy contribution ΔH_γ, a contribution due to solute–solvent interaction ΔH_ω, and an elastic strain energy contribution ΔH_ε. In this approximation, these terms have been combined linearly:

$$\Delta H_s = \Delta H_\gamma + \Delta H_\omega + \Delta H_\varepsilon \tag{9a}$$

In the limit of infinite dilution, these terms may be expressed as:

$$\Delta H_\gamma = (\gamma_2 - \gamma_1)A \tag{10a}$$

where the γ_i are the interfacial energies of the pure components i (1 = solvent, 2 = solute), and A is the area per mole of the solvent;

$$\Delta H_\omega = \frac{\Delta H_m}{Z^* X_1^b X_2^b} \tag{10b}$$

where ΔH_m is the enthalpy of mixing of the binary solution (assumed to be constant in a regular solution), Z^* is a number related to the coordination of atoms or ions in the interface, and

$$\Delta H_\varepsilon = -\frac{24\pi K G r_1 r_2 (r_2 - r_1)^2}{4G r_1 + 3K r_2} \tag{10c}$$

where K is the bulk modulus of the solute, G is the shear modulus of the solvent, and r_1 and r_2 are the atomic (or cation) radii of the solvent and solute species, respectively.

2.5. Electrostatic interactions in interfacial segregation

The simple model, described thus far, is appropriate for the description of segregation of isovalent solutes in ionic materials (as well as for simpler metallic and semiconducting systems), and was used some time ago with reasonable success for the interpretation of measurements of surface segregation of isovalent cations in metal oxides.[14–16] In the case of aliovalent solute segregation in ionic systems, however, it is necessary to account for additional energy changes associated with the electrostatic interaction between ionic charge difference and the internal potential, which result when an impurity ion in the bulk is exchanged with a solvent ion in the physical interface.

Thus, as far as the physical interface is concerned, the enthalpy of segregation of Eq. (9a) needs to be modified for aliovalent cations to include an electrostatic term:

$$\Delta H_s = \Delta H_\gamma + \Delta H_\omega + \Delta H_\varepsilon + \Delta H_\Phi \tag{9b}$$

where:

$$\Delta H_\Phi = -qe\Phi_\infty \tag{10d}$$

Here, q is the valence difference between the impurity and host cation.

The model approach described above is clearly oversimplified, as it assumes a linear combination of the various contributions to the driving force for segregation, and thus ignores possible interactions among the various terms that enter into Eq. (9b).[17] Nevertheless, it does identify the major terms which enter into the driving force for interfacial segregation in ionics. In addition, charge differences between an impurity and the solvent ions will also lead to electrostatic interactions with the space charge region. For the sake of completeness, we also show a schematic distribution of species in both the physical interface and the near-interface space charge region for the case of a NaCl-like crystal doped with a divalent cation in Fig. 3.

3. An approach for studying the effects of GB character on GB segregation

Some information is available on the relation between GB character and GB segregation, mainly in metallic sytems; however, this data has generally been gathered from studies of bicrystals grown so as to produce special

GBs (such as simple tilt and/or twist boundaries)[18–20] and is therefore limited in scope. Quite recently, the relative energies of grain boundaries in MgO have been determined as a function of all five macroscopic DoFs.[21] In this study, the five-dimensional DoF space was partitioned into 6561 distinct boundaries and these partitions were used to classify several million observed grain boundary plane segments. The acquisition of this large data set would not have been possible without the development of highly automated orientation imaging microscopy (OIM) to determine GB character. In addition to OIM, however, a large effort was required in order to measure the angles at which GBs meet at triple junctions, a necessary step in determining the relative GB energies. The approach proposed here also relies on OIM for the measurement of GB character. We therefore devote the following section to a brief description of that technique.

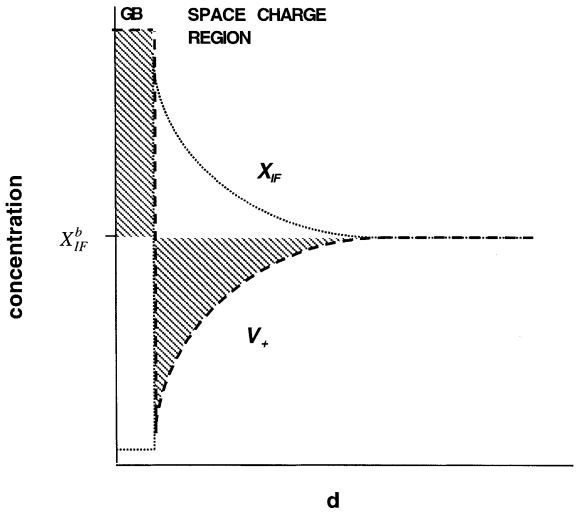

Fig. 3. Schematic of the near-GB half space of a NaCl-like ionic crystal doped with a divalent cation. X_{IF} (dotted line) is the concentration of unassociated divalent cations, V_+ (dashed line) the cation vacancy concentration, and X^b_{IF} the bulk concentration of unassociated divalent cations.

3.1. Measurement of GB character by OIM

OIM [22] allows the determination of the orientations of individual grains in a polycrystalline sample. OIM is performed in a specially modified scanning electron microscope. The basic modifications include the automated displacement of the sample stage and/or electron beam, so that electron backscattered diffraction patterns (EBSP) can be acquired at regularly-spaced points on the surface of a polycrystalline sample. A digital version of the EBSP is transmitted to a computer that performs image analysis and automatically returns the orientation of the point from which the EBSP originates. Every time a GB is crossed, the EBSP changes, and this information can also be used to identify the location of GBs. Thus, the three DoFs which describe the misorientation across the GBs in a polycrystalline sample can be determined automatically. If the two DoFs that describe GB inclination are also needed, then a serial sectioning process must be used. This involves the removal of a small known thickness of the sample surface by polishing. The changes in the locations of the GBs produced by polishing can be used to determine the GB inclination. A schematic of the EBSP acquisition process is displayed in Fig. 4.

3.2. Measurement of GB composition by auger electron spectroscopy

Auger electron spectroscopy (AES) is a powerful technique for the chemical analysis of surfaces.[23] A sample to be analyzed is introduced in an ultrahigh vacuum (UHV) chamber equipped with an electron gun

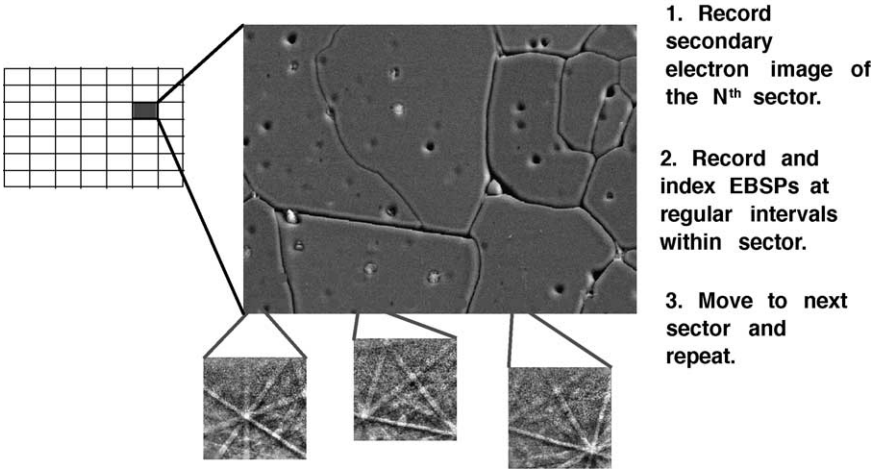

Fig. 4. Schematic of procedure used with OIM to determine the three angles which define GB misorientation. The sample is divided up into sectors, each sector is imaged, EBSP images are obtained on a grid in that sector, then the next sector is analyzed. This process is iterated until the sample surface is analyzed.

and an electron energy analyzer. The purpose of the UHV environment is to keep the surface clean of impurities which might be adsorbed onto the sample surface from the environment. An electron beam is directed towards the sample surface and the energies of the inelastically scattered electrons emanating from the sample are analyzed. Some of these electrons arise from so-called Auger transitions, which occur at energies that are element specific. The mean free paths of Auger electrons in the sample are quite short (0.2–1 nm), so that any Auger electrons detected in the vacuum, by the electron energy analyzer, originate from the region close to the sample surface, and carry with them information on near-surface chemical composition.

In order to obtain location-specific chemical analyses, a finely focussed electron beam must be used for Auger analysis. It must also be possible to image the surface and locate the beam at a pre-selected surface feature of interest. These types of capabilities are provided by a scanning Auger microscope (SAM). In this type of instrument, surface imaging is obtained by rastering the electron beam across the sample surface, as in a scanning electron microscope, with the image produced by detecting the emitted secondary electrons. The beam position can also be controlled so as to allow acquisition of Auger analyses at a point of interest on the surface.

As mentioned in Section 1, the chemical make-up of GBs can be obtained easily in samples prone to intergranular fracture, by analyzing the GB fracture surface. The sample can also be fractured in situ in the SAM so as to avoid contamination of the fracture surface by atmospheric gases. Once an intergranular fracture has been obtained, the electron beam can be moved from one GB to another on the fracture surface to obtain the compositions of all selected GBs.

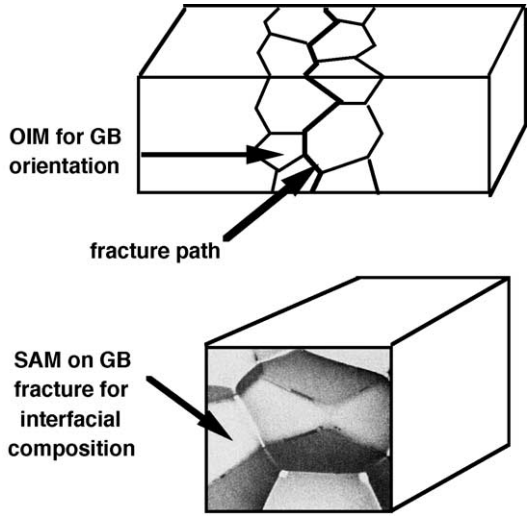

Fig. 5. Schematic of combined application of OIM and SAM on a given sample.

3.3. Combined OIM and SAM for correlation of GB character and GB composition

There are several ways of combining the two techniques mentioned above for obtaining a correlation between the character and equilibrium composition of GBs. Here we describe just one possible such approach.

The method is illustrated schematically in Fig. 5. The sample used is a rod of rectangular cross-section. As a first step, OIM is performed to determine the misorientation of all boundaries on the sample surfaces, and images of these surfaces are taken at a suitable magnification. (The sample could be notched so as to fix the general area in which fracture will occur, and thus limit the area over which OIM analysis needs to be performed.) If all five macroscopic DoFs are required, serial sectioning may be applied, and OIM analysis repeated. As a second step, the sample is introduced into a SAM and fractured. All GBs which intercept the original sample surface (where OIM has previously been employed to characterize the GBs) are then analyzed by AES. The GB composition information can thus be connected with the character of that boundary.

Experiments of this type are currently being started at Carnegie Mellon University. At this time, the SAM component of the work is being performed manually. Longer range, the SAM component of such a combined approach would need to be automated in order to acquire GB composition information at a rate comparable to those of the OIM technique. Some preliminary results are given in the following section.

3.4. Preliminary results

In view of the extensive studies of GB character that have recently been carried out in MgO,[21] this material has been selected for initial GB segregation studies. According to the literature,[15,24,25] Ca, Sr, Ba, Sc, and Si have been identified as segregant species in MgO, although Ca segregation has been the most studied case.

In this work, a polycrystalline MgO specimen was prepared from (99.9%) MgO carbonate containing Ca impurities. After calcination, the powder was cold pressed into the form of a plate, then sintered in air at 1600 °C for 15 h. Final Ca content was determined by inductively coupled plasma emission spectrometry (ICP–AES) to be 3670 ± 180 ppm. Other impurities were present in lower concentrations. Grain size was in the range of 50–100 μm.

Fig. 6 is an SEM micrograph of one face of the sample after fracture. The fracture contains both intergranular regions as well as regions of cleavage. AES analysis was performed on selected GBs (indicated in Fig. 7a) in a scanning Auger microprobe (Perkin Elmer PHI 600) under ultrahigh vacuum ($1.5\ 10^{-10}$ MPa) at a beam energy of 3 kV.

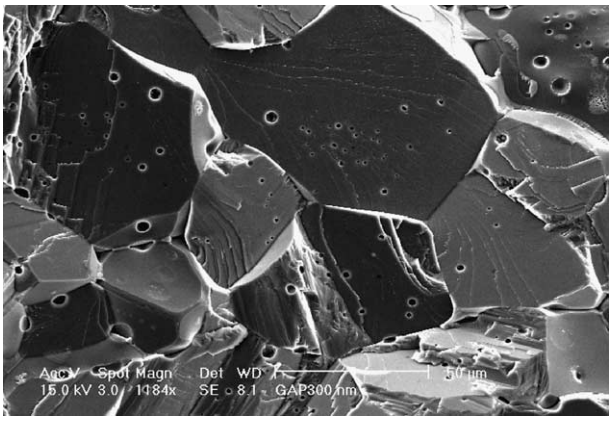

Fig. 6. SEM photomicrograph of fracture surface of MgO specimen containing 0.3% Ca showing regions of cleavage (with no impurity) and interganular fracture (with segregation).

Table 1
Measured segregation at the points indicated on Fig. 7a

Point	$X^{\varphi}_{Ca}/X^{\varphi}_{Mg}$	$X^{\varphi}_{Ca}/X^{b}_{Ca}$
P1	0.03	10
P2	0	–
P3	0.27	71
P4	0.25	67
P5	0	–

A typical AES spectrum for an MgO GB is shown in Fig. 7b. The elements systematically detected at various points on the fracture surface were O, Mg and C. A Ca peak of readily observable intensity was found only at some of the locations identified in Fig. 7a. The Ca surface concentration at these points is reported in Table 1 as the ratio of Ca to Mg mole fractions at the surface, $X^{\varphi}_{Ca}/X^{\varphi}_{Mg}$, as well as the Ca enrichment factor, $X^{\varphi}_{Ca}/X^{b}_{Ca}$. The table shows that some points (P2 and P5) display no detectable Ca, indicating that these points are probably located on cleavage surfaces. Other points show Ca enrichments ranging from 10 to 70.

Thus, the first objective of our study, namely: to establish that segregation of Ca to boundaries in MgO does indeed vary from one GB to another, has been accomplished. Plans for future work include a determination of conditions which will yield essentially complete intergranular fracture, and the deliberate doping of MgO with CaO so as to increase the average Ca concentration at GBs. Finally, it will be necessary to implement and perfect the procedures for combining OIM and AES measurements.

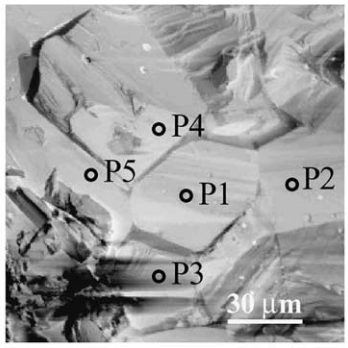

(a)

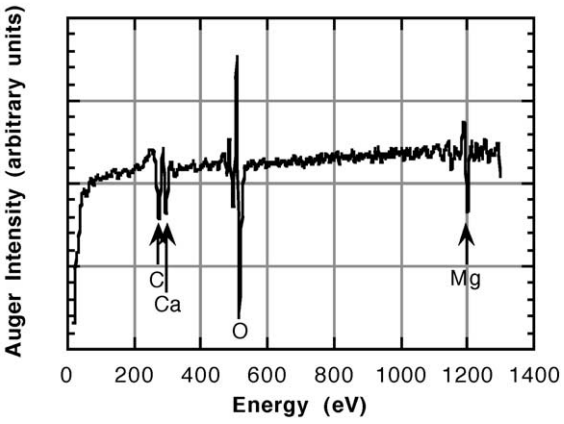

(b)

Fig. 7. (a) SAM micrograph of fracture surface of the sample shown in Fig. 6, indicating points at which AES analysis was performed (AES results are summarized in Table 1). (b) Representative AES spectrum from point P1 in (a).

Acknowledgements

P.W. and F.P. wish to acknowledge with thanks support of this research by NSF under grant DMR 9820169. Partial support by the MRSEC program of the National Science Foundation under Award Number DMR-0079996 is also acknowledged.

References

1. Gibbs, J. W., *The Scientific Papers of J. Willard Gibbs*. Vol. 1, Dover NY, 1961.
2. Krakauer, B. W. and Seidman, D. N., Systematic procedures for atom-probe field-ion microscopy studies of grain boundary segregation. *Rev. Sci. Instrum*., 1992, **63**, 4071–4079.
3. Bouchet, D., Colliex, C., Flora, P., Krivanek, O., Mory, C. and Tencé, M., Analytical electron microscopy at the atomic level with parallel electron-energy spectroscopy. *Microsc. Microanal. Microstruct*., 1990, **1**, 443–454.
4. Thompson, A. M., Soni, K. K., Chan, H. M., Harmer, M. P., Williams, D. B., Chabala, J. M. and Levi-Setti, R., Dopant distributions in rare-earth-doped alumina. *J. Am. Ceram. Soc*., 1997, **80**, 373–376; Gavrilov, K. L., Bennison, S. J., Mikeska, K. R., Chabala, J. M. and Levi-Setti, R., Silica and magnesia dopant distributions in alumina by high-resolution scanning secondary ion mass spectrometry. *Ibid*., 1999, **82**, 1001–1008.
5. Low, J. R. Jr., Impurities, interfaces and brittle fracture. *Trans. Met. Soc. AIME*, 1969, **245**, 2481–2491.
6. Frenkel, J., *Kinetic Theory of Liquids*, Dover, NY, 1955.

7. Lehovec, K., Space-charge layer distribution of lattice defects at the surface of ionic crystals. *J. Chem. Phys*., 1953, **21**, 1123–1128.
8. Kliewer, K. L. and Koehler, J. S., Space charge in ionic crystals—1. General approach with applications to NaCl. *Phys. Rev. A*, 1965, **140**, 1226–1240.
9. Poeppel, R. B. and Blakely, J. M., Origin of space charge potentials in ionic crystals. *Surface Sci*., 1969, **15**, 507–523.
10. Blakely, J. M. and Danyluk, S., Space charge regions at silver halide surfaces: effects of divalent impurities and halogen pressure. *Surface Sci*., 1973, **40**, 37–60.
11. Desu, S. B. and Payne, D. A., Interfacial segregation in perovskites: 1 Theory. *J. Am. Ceram. Soc*., 1990, **73**, 3391–3397.
12. Defay, R., Prigogine, I., Bellmans, A. and Everett, D. H., *Surface Tension and Adsorption*. Wiley, New York, 1966.
13. Wynblatt, P. and Ku, R. C., Surface segregation in alloys. In *Interfacial Segregation*, ed. W. C. Johnson and J. M. Blakely. ASM, Metals Park OH, 1979, pp. 115–136.
14. Wynblatt, P. and McCune, R. C., Chemical aspects of equilibrium segregation to ceramic interfaces. In *Surfaces and Interfaces in Ceramic and Ceramic-Metal Systems*, ed. J. A. Pask and A. G. Evans. Plenum, NY, 1981, pp. 83–95.
15. Wynblatt, P. and McCune, R. C., Calcium segregation to a magnesium oxide (100) surface. *J. Am. Ceram. Soc*., 1983, **66**, 111–117.
16. Wynblatt, P. and McCune, R. C., Surface segregation in metal oxides. In *Surface and Near-Surface Chemistry of Oxide Materials*, ed. J. Nowotny and L.-C. Dufour. Elsevier, Amsterdam, 1988, pp. 247–279.
17. Yan, M. F., Cannon, R. M. and Bowen, H. K., Space charge, elastic field and dipole contributions to equilibrium solute segregation at interfaces. *J. Appl. Phys*., 1983, **54**, 764–778.
18. Lejcek, P. and Hoffmann, S., Thermodynamics and structural aspects of grain boundary segregation. *Crit. Rev. Sol. State Mater. Sci*., 1995, **20**, 1–85 (and references therein).
19. Roshko, A. and Kingery, W. D., Segregation at special boundaries in MgO. *J. Am. Ceram. Soc*., 1985, **68**, C331–C333.
20. Hall, E. L., Imeson, D. and Vander Sande, J. B., On producing high-spatial-resolution composition profiles via scanning-transmission electron microscopy. *Phil. Mag*., 1981, **A43**, 1569–1585.
21. Saylor, D. M., Morawiec, A. and Rohrer, G. S., The distribution and energies of grain boundaries as a function of five degrees of freedom. *J. Am. Ceram. Soc*., 2002, **85**, 3081–3083.
22. Adams, B. L., Wright, S. I. and Kunze, K., Orientation imaging - the emergence of a new microscopy. *Metall. Trans*, 1993, **24A**, 819–831.
23. Briggs, D. and Seah, M. P., *Practical Surface Analysis by Auger and X-ray Photoelectron Spectroscopy*. John Wiley and Sons, New York, 1984.
24. Chiang, Y. M., Henriksen, A. F. and Kingery, W. D., Characterization of grain-boundary segregation in MgO. *J. Am. Ceram. Soc*., 1981, **64**, 385–389.
25. Tasker, P. W., Colburn, E. A. and Mackrodt, W. C., Segregation of isovalent impurity cations at the surfaces of MgO and CaO. *J. Am. Ceram. Soc*., 1985, **68**, 74–80.